INTERNATIONAL JOURNAL OF AGRICULTURE & BIOLOGY
ISSN Print: 1560–8530; ISSN Online: 1814–9596
18–0037/2018/20–9–1961–1969
DOI: 10.17957/IJAB/15.0715
http://www.fspublishers.org

Full Length Article

Proteomic Changes in Urediospores of *Puccinia striiformis* f. sp. *tritici* After UV-B Radiation

Yaqiong Zhao[1†], Pei Cheng[1†], Tingting Li[1†] and Haiguang Wang[1*]
[1]*Department of Plant Pathology, China Agricultural University, Beijing 100193, China*
[*]For correspondence: wanghaiguang@cau.edu.cn
[†]Contributed equally to this work and listed as the first author

Abstract

Virulence variation in *Puccinia striiformis* f. sp. *tritici* (*Pst*) that causes wheat stripe rust is the most important reason for the resistance breakdown of existing resistant wheat cultivars. To explore the mechanism of variation of *Pst* induced by UV-B radiation, the proteomic changes of urediospores of three Chinese physiological races of *Pst* including CYR31, CYR32 and CYR33 after UV-B radiation were profiled using the isobaric tags for relative and absolute quantification (iTRAQ) technology in combination with LC-MS/MS. The results showed that 2,136 proteins were identified from the UV-B irradiated urediospores and the corresponding controls (non-UV-B irradiated urediospores) of the three physiological races. Quantitative analysis showed that 43, 45 and 35 differentially expressed proteins were obtained in the UV-B irradiated urediospores of CYR31, CYR32 and CYR33 compared to the corresponding controls. The results obtained using Gene Ontology (GO) analysis, Cluster of Orthologous Groups (COG) analysis and Kyoto Encyclopedia of Genes and Genomes (KEGG) pathway analysis demonstrated that the acquired differentially expressed proteins were mainly involved in energy metabolism, substance metabolism and DNA biosynthesis. This study provided a basis for further investigations into the virulence variation mechanisms of *Pst* caused by UV-B radiation. © 2018 Friends Science Publishers

Keywords: *P. striiformis*; Wheat stripe rust; UV-B radiation; iTRAQ; Differential proteomics

Introduction

Stripe rust caused by *Puccinia striiformis* f. sp. *tritici* (*Pst*), is an important disease in wheat worldwide (Li and Zeng, 2002; Line, 2002; Chen *et al*., 2014; Wang *et al*., 2014). *Pst* urediospores can be spread over long distances with air flows, and after deposition on wheat leaves, they can infect leaves and induce disease epidemics, resulting in severe wheat yield losses. Changes in ultraviolet-B (UV-B) (280–320 nm) radiation, carbon dioxide and ozone in the atmosphere caused by global climate change have potential impacts on plant diseases (Manning and Tiedemann, 1995). In particular, UV-B radiation may have impacts on the survival and genetic variation of *Pst* in high-altitude areas with high-intensity UV-B radiation and in processes of *Pst* long-distance dispersal with upper air flows (Li and Zeng, 2002; Cheng *et al*., 2014).

UV-B radiation can affect plants in many ways, such as gene expression (Inostroza-Blancheteau *et al*., 2014; Trentin *et al*., 2015), growth (Teramura and Sullivan, 1994) and biological morphology (Brosché and Strid, 2000; Cuadra *et al*., 2010). It can affect plant pathogens in germinability of pathogen spores (Willocquet *et al*., 1996; Costa *et al*., 2012; Cheng *et al*., 2014; Braga *et al*., 2015), extension and elongation of germ tubes (Costa *et al*., 2012; Braga *et al*., 2015), hyphal growth (Willocquet *et al*., 1996; Fourtouni *et al*., 1998), and so on, thus affecting the occurrence of plant diseases. UV radiation affected the pathogenicity of *Pst* (Jing *et al*., 1993; Cheng *et al*., 2014), and virulence mutant strains of *Pst* from the UV-irradiated *Pst* urediospores were obtained (Shang *et al*., 1994; Huang *et al*., 2005; Wang *et al*., 2009). UV radiation is one way to induce the virulence variation in *Pst* (Shang *et al*., 1994; Huang *et al*., 2005; Wang *et al*., 2009; Kang *et al*., 2015). Therefore, further studies on the mechanism of virulence variation in *Pst* induced by UV-B radiation can provide a basis for exploring the reasons for resistance breakdown in the existing resistant wheat cultivars.

Differential proteomics aims to study differentially expressed proteins (DEP) and to explore the effects of external factors on organisms (Pandey and Mann, 2000). The combination of two-dimensional gel electrophoresis (2-DE) and mass spectrometry (MS) techniques has promoted the development of proteomics. Furthermore, the emergence of non-gel-based separation techniques has accelerated the development and application of proteomics. The isobaric tags for relative and absolute quantification (iTRAQ) technique, a non-gel-based, relative quantitative technique with high sensitivity for proteomics, has been widely used in high-throughput screening of differential proteins in

To cite this paper: Zhao, Y., P. Cheng, T. Li and H. Wang, 2018. Proteomic changes in urediospores of *Puccinia striiformis* f. sp. *tritici* after UV-B radiation. *Int. J. Agric. Biol*., 20: 1961–1969

many fields, such as in plants (Zhu *et al*., 2010), microorganisms (Redding *et al*., 2006) and plant-pathogen interactions (Rosen *et al*., 2003; Fu *et al*., 2016). In terms of *Pst*-wheat interactions, most relevant studies (Liang *et al*., 2007; Ma *et al*., 2009; Maytalman *et al*., 2013; Yang *et al*., 2016) focused on the differential expression of host proteins after wheat hosts were infected with *Pst* for screening proteins associated with the interactions. However, few studies on the proteomics of stripe rust pathogen during plant-*Pst* interactions have been reported. Demirci *et al*. (2016) conducted proteome profiling of wheat and *Pst* during their compatible interaction.

Few reports have focused on the proteomics of urediospores of plant pathogenic rust fungi (Cooper *et al*., 2007; Luster *et al*., 2010; Zhao *et al*., 2016). A study on profiling the changes in the proteome of germinating urediospores of *Phakopsora pachyrhizi* was conducted by Luster *et al*. (2010) using a 2-DE and MS approach. The differential proteome of *Pst* urediospores before and after germination was studied by Zhao *et al*. (2016) using iTRAQ and MS techniques. These studies provided a basis for exploring the molecular mechanisms of rust fungal urediospore infection into plants. An increasing number of studies to investigate the proteomic changes of plants (Trentin *et al*., 2015) or microorganisms (Kramer *et al*., 2015) induced by UV radiation have been performed, indicating that the biological effects of UV radiation have caused widespread concern.

In this study, using iTRAQ technology, DEP of three Chinese physiological races of *Pst* (CYR31, CYR32 and CYR33) between UV-B irradiation urediospores and non-UV-B irradiation urediospores were investigated to profile the proteomic changes of *Pst* induced by UV-B radiation and to provide support for exploring genetic variation mechanisms of *Pst*.

Materials and Methods

Pst Multiplication

Three physiological races of *Pst* including CYR31, CYR32 and CYR33 were used in this study. Each physiological race was isolated from a single uredium. Using the method described by Cheng *et al*. (2014), multiplication of the urediospores of each *Pst* physiological race was carried out on Mingxian 169 (a wheat cultivar susceptible to all known Chinese physiological races of *Pst*).

Screening for UV-B Radiation Levels

In this study, a UV-B radiation intensity of 200 μw/cm^2 was used for treatment of *Pst* urediospores according to the UV-B radiation intensities previously measured in the epidemic areas in China during the epidemic of wheat stripe rust (Cheng *et al*., 2014). The highest variation probability of *Pst* urediospores could be achieved when the relative lethal rate of the urediospores was 90% under UV-B radiation (Jing *et al*., 1993; Huang *et al*., 2005; Wang *et al*., 2009). Therefore, for each *Pst* physiological race, the radiation time required for a 90% relative lethal rate of urediospores at the UV-B intensity of 200 μw/cm^2 was screened using the method shown as follows.

First, 30 mg of fresh urediospores of CYR31, CYR32 or CYR33 collected from the diseased wheat seedlings were evenly scattered in a 10 cm diameter Petri dish. Using the method described by Cheng *et al*. (2014), UV-B radiation of *Pst* urediospores in the Petri dish was performed with the UV-B intensity of 200 μw/cm^2 for some time, and then the germination rate of the urediospores was determined. The urediospores of the same physiological race without UV-B radiation were treated as the control. Based on the germination rates of the irradiated urediospores and the urediospores of the control, the relative germination rate of the irradiated urediospores was calculated and the relative lethal rate after UV-B radiation was obtained. The radiation time at which a relative lethal rate of 90% was achieved, was regarded as the optimal time for UV-B radiation. After screening based on a set of time gradients for UV-B radiation, the optimal radiation time for each physiological race was finally obtained. For CYR31, CYR32 and CYR33, the optimal radiation times were 185, 200 and 190 min, respectively. The corresponding UV-B radiation dose at the optimal radiation time for each physiological race was recorded as LD_{90} (i.e., 90% lethal dose).

Protein Extraction and iTRAQ Labeling

From the UV-B irradiated and non-UV-B irradiated urediospores of the three *Pst* physiological races, the corresponding proteins were extracted. To conveniently express the urediospore samples of CYR31, CYR32 and CYR33 after irradiation with the UV-B radiation doses of LD_{90}, the corresponding samples were recorded as $CYR31LD_{90}$, $CYR32LD_{90}$, and $CYR33LD_{90}$, respectively. Similarly, the non-UV-B irradiated urediospore samples of CYR31, CYR32 and CYR33 were recorded as CYR31CK, CYR32CK, and CYR33CK, respectively. First, each urediospore sample (30 mg) was combined with 500 μL of lysis buffer containing one m*M* phenylmethanesulfonyl fluoride, two m*M* ethylenediaminetetraacetic acid, eight *M* urea, ten m*M* dithiothreitol (DTT), and 30 m*M* 4-(2-hydroxyethyl)-1-piperazineethanesulfonic acid. After sonication for 5 min, each sample was centrifuged at 4℃ and 20,000 g for 30 min. The collected supernatant was combined with DTT to a final concentration of ten m*M*. After incubation in a water bath at 56℃ for 1 h, the supernatant was rapidly mixed with iodoacetamide to a final concentration of 55 m*M* and incubated for 1 h in the dark. The supernatant was mixed with fourfold volume of chilled acetone, precipitated at -20℃ for more than three hours, and centrifuged for 30 min at 4℃ and 20,000 g. Dissolving the protein pellet with 300 μL of digestion buffer [50% triethylammonium bicarbonate (TEAB) and 0.1% sodium

dodecyl sulfate (SDS)] was performed. After sonication for 3 min and centrifugation for 30 min at 4℃ and 20,000 g, the supernatant was finally collected. Determination of the protein concentration in the supernatant was conducted using Bradford assay.

After protein extraction, an aliquot (100 μg) from each of the six protein samples was transferred to a new clean centrifuge tube by adding TEAB (0.1% SDS) to make each sample at the same volume. The proteins in the tube were digested by adding 3.3 μL of trypsin (one μg/μL) and incubated in a water bath at 37°C for 24 h. After adding with one μL of trypsin (one μg/μL), the mixture in the tube was incubated in a waterbath at 37°C for 12 h and lyophilized. Peptides were dissolved by adding 30 μL of TEAB (ddH_2O:TEAB=1:1, v/v). iTRAQ labeling of peptides was conducted using an iTRAQ® Reagent-8Plex Multiplex Kit (Applied Biosystem, Foster City, CA, USA). Peptides from CYR31CK, $CYR31LD_{90}$, CYR32CK, $CYR32LD_{90}$, CYR33CK and $CYR33LD_{90}$ were labeled with the isobaric tags 113, 114, 115, 118, 119 and 121, respectively.

The dried, labeled peptide mixture was dissolved with buffer A (25% acetonitrile (ACN), ten m*M* of KH_2PO_4, pH 3.0) and centrifuged for 15 min at 15,000 g. Then the labeled peptides in the liquid supernatant were eluted at a flow rate of one mL/min using a Phenomenex Luna SCX 100A column with a HPLC system (Thermo Fisher Scientific, Waltham, MA, USA). Before strong cation exchange fractionation, buffer A was used to balance the system for 10–20 min at a flow rate of one mL/min. The HPLC gradient consisted of 100% buffer A for 40 min, from 0 to 5% buffer B (25% ACN, two *M* KCl, 10 m*M* of KH_2PO_4, pH 3.0) for 1 min, from 5 to 30% buffer B for 20 min, from 30 to 50% buffer B for 5 min, 50% buffer B for 5 min, from 50 to 100% buffer B for 5 min and 100% buffer B for 10 min. The eluted peptides were desalted with a Strata-X C18 column (Phenomenex, Torrance, CA, USA) and evaporated to dryness at a low temperature using a vacuum centrifuge.

Nano LC-MS/MS Analysis

The desalted, dried peptides were dissolved with solvent A (0.1% formic acid (FA) in H_2O). On a C18 chromatographic column (75 μm×100 mm, five μm particle size, 300 Å pore size, Agela Technologies), the dissolved peptides were separated at a flow rate of 400 nL/min with a gradient of 5% solvent B (0.1% FA in ACN) for 10 min, from 5 to 30% solvent B for 30 min, from 30 to 60% solvent B for 5 min, from 60 to 80% solvent B for 3 min, 80% solvent B for 7 min, from 80 to 5% solvent B for 3 min and 5% solvent B for 7 min. Using a Q-Exactive mass spectrometer (Thermo Fisher Scientific, Waltham, MA, USA), the separated peptides were detected in the positive ion mode. The MS scan range was 350 Da to 2,000 Da. Based on the m/z of precursor ions, the scan range was automatically selected for MS2 scans with a resolution of 17,500. The capillary temperature was 320℃. The ion source voltage applied was 1,800 V. The high-energy collision dissociation operating mode was used. Raw MS/MS data were input into Proteome Discoverer 1.3 (Thermo Fisher Scientific) and screened with 350–6,000 Da as the MS mass range, 10 as the minimum threshold of peaks in the MS/MS spectrum and 1.5 as the signal-to-noise ratio (S/N).

Proteomic Data Analyses

Protein identification and quantification were carried out using Mascot 2.3.0 (Matrix Science, London, UK), searching against the uniprot_Basidiomycota database (http://www.uniprot.org/proteomes/?query=Basidiomycota & sort=score). The data were searched with carbamidomethyl (C) as the fixed modification, oxidation (M), Gln-> pyro-Glu (N-term Q), iTRAQ eight plex (K), iTRAQ eight plex (Y) and iTRAQ eight plex (N-term) as the variable modifications, 15 ppm as the peptide tolerance, 20 mDa as the MS/MS tolerance, one as the max missed cleavages, and trypsin as the digest enzyme. For protein quantitative analysis, the protein ratio type was set as the median, minimum peptides were set as one, and the normalization method applied was the median. Proteins with the *P*-values less than 0.05 and the fold changes more than 1.5 were identified as DEP (Briolant *et al*., 2010).

The Gene Ontology (GO) annotations of the identified proteins were conducted using the blast2go program (http://www.blast2go.com/b2ghome/about-blast2go) (Conesa *et al*., 2005). The Cluster of Orthologous Groups of Proteins (COG) annotations were obtained through a web server WebMGA (http://weizhong-lab.ucsd.edu/metagenomic-analysis/server/cog/) (Wu *et al*., 2011). The annotations of the identified DEP were conducted at the biological pathway level using the Kyoto Encyclopedia of Genes and Genomes (KEGG) program. KOBAS 2.0 software was used to compare the similarity of the protein sequences and to annotate the pathways.

Results

Overview of the Proteomic Data

By searching against the Basidiomycota protein database in UniProt (false discovery rate < 1%), 42,740 spectra from all 327,427 spectra were matched. In total, 7,992 peptides and 2,136 proteins were obtained. There were 43, 45 and 35 DEP in the UV-B irradiated urediospores of CYR31, CYR32 and CYR33 compared to the corresponding controls, as shown in a Venn diagram drawn using the Venny 2.1 tool (http://bioinfogp.cnb.csic.es/tools/venny/index.html) (Fig. 1). There were 26, 20 and 14 up-regulated proteins and 17, 25 and 21 down-regulated proteins in the three UV-B radiation treatments $CYR31LD_{90}$, $CYR32LD_{90}$, and $CYR33LD_{90}$, respectively. Most of DEP differed between

the combinations—including $CYR31LD_{90}$ VS CYR31CK, $CYR32LD_{90}$ VS CYR32CK, and $CYR33LD_{90}$ VS CYR33CK—and only seven proteins were common for all combinations, indicating that there were different effects of UV-B radiation on the urediospores of each *Pst* physiological race.

COG Annotations of *Pst* Proteome

Using the COG function annotation classification system, 2,136 proteins acquired were functionally matched and annotated. As shown in Fig. 2, all matched proteins of the three physiological races were divided into 25 categories that were represented from A to Z, and the number of involved proteins in each category was also presented. Proteins were mainly involved in the following four categories: "[J] translation, ribosomal structure and biogenesis" (275 proteins), "[O] posttranslational modification, protein turnover, chaperones" (267 proteins), "[C] energy production and conversion" (212 proteins), and "[U] intracellular trafficking, secretion, and vesicular transport" (174 proteins).

GO Annotations, COG Functional Classification and KEGG Pathway Enrichment Analysis of DEP

The GO annotations of DEP acquired in the three UV-B radiation treatments $CYR31LD_{90}$, $CYR32LD_{90}$, and $CYR33LD_{90}$ were conducted, and of these, 61 proteins were annotated and classified into "cellular component" (CC), "molecular function" (MF), and "biological process" (BP) (Fig. 3). Among the 61 proteins, 47 belonged to each of the three categories; the number of DEP involved in each combination of two categories, namely, CC/MF, CC/BP or MF/BP, were three, three or one, respectively; and the number of unique proteins for CC, MF and BP were one, three and three, respectively.

The COG functional annotations of DEP acquired in the three UV-B radiation treatments of $CYR31LD_{90}$, $CYR32LD_{90}$, and $CYR33LD_{90}$ were performed. Among these DEP, 49 proteins were up-regulated and annotated as listed in Table 1 and 56 proteins were down-regulated and annotated as listed in Table 2.

KEGG analysis was carried out to annotate the identified DEP at the pathway level ($P < 0.05$). Based on the KEGG pathway enrichment analysis, three, two and eight pathways listed in Table 3 were achieved from each of the three treatment combinations, including $CYR31LD_{90}$ VS CYR31CK, $CYR32LD_{90}$ VS CYR32CK, and $CYR33LD_{90}$ VS CYR33CK, respectively.

Discussion

In this study, 2,136 proteins were identified from the UV-B irradiated and non-UV-B irradiated urediospores of the three Chinese physiological races of *Pst*. The results indicated

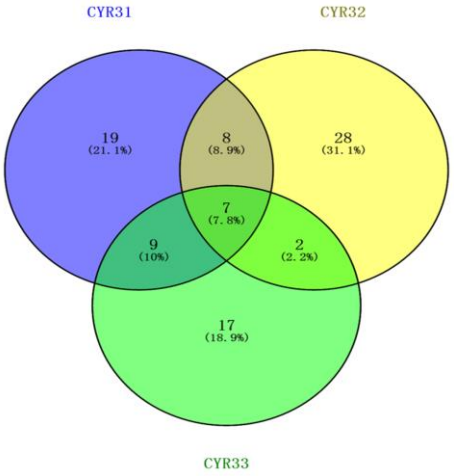

Fig. 1: The overlap among the differentially expressed proteins in the urediospores of the three *Pst* physiological races (CYR31, CYR32 and CYR33) analyzed by using iTRAQ technology before and after UV-B radiation

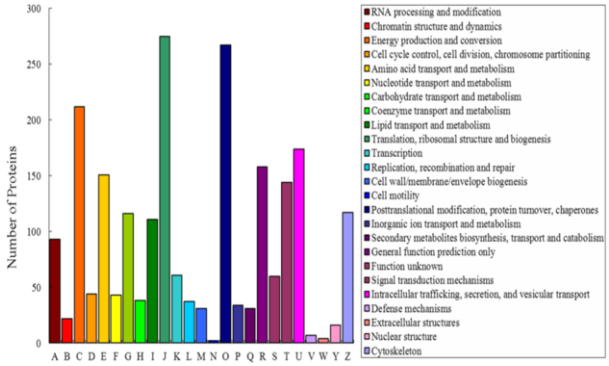

Fig. 2: COG classification of *P. striiformis* f. sp. *tritici* proteome

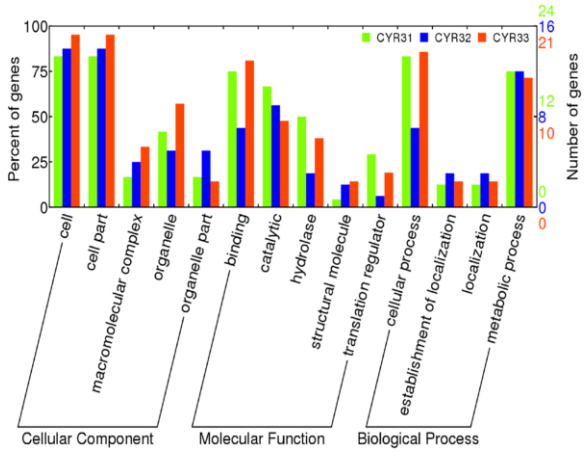

Fig. 3: Gene ontology (GO) classification of the differentially expressed proteins in urediospores of the three physiological races of *Puccinia striiformis* f. sp. *tritici*

Table 1: Up-regulated differentially expressed proteins in the urediospores of the three *Pst* physiological races including of CYR31, CYR32 and CYR33 after UV-B radiation

COG functional classification	Accession	Description	Treatment combination	Fold change
Information storage and processing				
[A]RNA processing and modification	H6QQ22	Putative uncharacterized protein	CYR33LD$_{90}$ VS CYR33CK	2.31
	J3Q5E8	Uncharacterized protein	CYR31LD$_{90}$ VS CYR31CK	2.44
			CYR33LD$_{90}$ VS CYR33CK	2.35
	U5GYG7	Uncharacterized protein	CYR32LD$_{90}$ VS CYR32CK	1.53
[B]Chromatin structure and dynamics	M5FWC9	Histone H2A	CYR31LD$_{90}$ VS CYR31CK	2.30
[J]Translation, ribosomal structure and biogenesis	A4KBU8	Translation elongation factor 1 alpha	CYR31LD$_{90}$ VS CYR31CK	1.77
	A8PX11	Putative uncharacterized protein	CYR32LD$_{90}$ VS CYR32CK	2.20
	C0K1C3	Transcription elongation factor 1-alpha	CYR31LD$_{90}$ VS CYR 31CK	2.21
	E3JQ18	60S ribosomal protein L36	CYR32LD$_{90}$ VS CYR32CK	1.58
	I4Y6G4	Elongation factor 1-alpha	CYR31LD$_{90}$ VS CYR31CK	1.89
	I4YGJ3	Ribosomal protein L15	CYR32LD$_{90}$ VS CYR32CK	1.99
	J3Q8W4	Uncharacterized protein	CYR32LD$_{90}$ VS CYR32CK	1.80
	J3QH44	Uncharacterized protein	CYR32LD$_{90}$ VS CYR32CK	1.78
	M7WTM4	Translation initiation factor eIF-4A	CYR31LD$_{90}$ VS CYR31CK	1.84
	Q5EG81	Translation elongation factor EF1-alpha	CYR31LD$_{90}$ VS CYR31CK	2.09
	S8FN91	Uncharacterized protein	CYR32LD$_{90}$ VS CYR32CK	1.55
	U3L266	Elongation factor 1-alpha	CYR31LD$_{90}$ VS CYR31CK	2.34
	V2XVD8	60s ribosomal protein l34-b	CYR32LD$_{90}$ VS CYR32CK	2.24
[L]Replication, recombination and repair	E3KKF8	Putative uncharacterized protein	CYR31LD$_{90}$ VS CYR31CK	1.87
Cellular processes and signaling				
[M]Cell wall/membrane/envelope biogenesis	M5G8J5	L-glutamine D-fructose 6-phosphate amidotansferase	CYR31LD$_{90}$ VS CYR31CK	1.65
[O]Posttranslational modification, protein turnover, chaperones	A8NE72	SCF ubiquitin ligase	CYR31LD$_{90}$ VS CYR31CK	1.60
	A7KJS2	14-3-3 protein	CYR31LD$_{90}$ VS CYR31CK	1.89
	E6ZRI2	Proteasome subunit beta type	CYR32LD$_{90}$ VS CYR32CK	1.58
	J3PMB0	Uncharacterized protein	CYR32LD$_{90}$ VS CYR32CK	1.61
	K5WSF5	Uncharacterized protein	CYR31LD$_{90}$ VS CYR31CK	1.52
	M9LXF6	Succinyl-coa synthetase, alpha subunit	CYR31LD$_{90}$ VS CYR31CK	1.61
[U]Intracellular trafficking, secretion, and vesicular transport	E3JQG7	ER lumen protein retaining receptor	CYR33LD$_{90}$ VS CYR33CK	1.52
	M7X4F7	Protein transport protein SEC23	CYR31LD$_{90}$ VS CYR31CK	1.54
			CYR33LD$_{90}$ VS CYR33CK	2.75
[D]Cell cycle control, cell division, chromosome partitioning	E3JX07	Putative uncharacterized protein	CYR33LD$_{90}$ VS CYR33CK	2.19
[Z]Cytoskeleton	B0LC31	Beta-tubulin 1	CYR33LD$_{90}$ VS CYR33CK	2.66
	G7DSE9	Uncharacterized protein	CYR33LD$_{90}$ VS CYR33CK	1.88
Metabolism				
[C]Energy production and conversion	E3K6X4	Isocitrate dehydrogenase	CYR31LD$_{90}$ VS CYR31CK	1.56
	J3PS85	Uncharacterized protein	CYR31LD$_{90}$ VS CYR31CK	1.69
	K5VWF0	Uncharacterized protein	CYR32LD$_{90}$ VS CYR32CK	1.54
			CYR33LD$_{90}$ VS CYR33CK	1.98
	W4K8P5	NADH:ubiquinone oxidoreductase	CYR31LD$_{90}$ VS CYR31CK	1.63
[F]Nucleotide transport and metabolism	E3KYR7	Thymidylate synthase	CYR31LD$_{90}$ VS CYR31CK	1.52
[G]Carbohydrate transport and metabolism	J3Q3W0	Uncharacterized protein	CYR31LD$_{90}$ VS CYR31CK	3.27
			CYR32LD$_{90}$ VS CYR32CK	2.02
	M7X689	Phosphoglycerate kinase	CYR33LD$_{90}$ VS CYR33CK	2.48
[H]Coenzyme transport and metabolism	F4RPZ7	Putative uncharacterized protein	CYR32LD$_{90}$ VS CYR32CK	2.25
[I]Lipid transport and metabolism	E3JRQ6	Acetyl-CoA acyltransferase 2	CYR33LD$_{90}$ VS CYR33CK	1.51
Poorly characterized				
[S]Function unknown	E3K9F8	Putative uncharacterized protein	CYR31LD$_{90}$ VS CYR31CK	1.60
[R]General function prediction only	J3PT86	Uncharacterized protein	CYR31LD$_{90}$ VS CYR31CK	1.92
			CYR32LD$_{90}$ VS CYR32CK	1.82
No annotation	E3KXV4	Phospho-2-dehydro-3-deoxyheptonate aldolase	CYR31LD$_{90}$ VS CYR31CK	1.82
	F4R846	Putative uncharacterized protein	CYR31LD$_{90}$ VS CYR31CK	7.14
			CYR32LD$_{90}$ VS CYR32CK	1.52
	J3Q8U2	Uncharacterized protein	CYR31LD$_{90}$ VS CYR31CK	2.25
			CYR32LD$_{90}$ VS CYR32CK	1.93
			CYR33LD$_{90}$ VS CYR33CK	2.06
	J3PSZ8	Uncharacterized protein	CYR32LD$_{90}$ VS CYR32CK	1.92
	J3PZX9	Uncharacterized protein	CYR32LD$_{90}$ VS CYR32CK	1.60
			CYR33LD$_{90}$ VS CYR33CK	2.16
	K5XEZ5	Uncharacterized protein	CYR32LD$_{90}$ VS CYR32CK	1.66
			CYR33LD$_{90}$ VS CYR33CK	2.71
	V2YR52	Uncharacterized protein	CYR31LD$_{90}$ VS CYR31CK	2.20
			CYR33LD$_{90}$ VS CYR33CK	62.50
	W4JNS8	Uncharacterized protein	CYR32LD$_{90}$ VS CYR32CK	1.57

that each of the three *Pst* physiological races had different responses to UV-B radiation. According to Cheng *et al.* (2014), the sensitivity to UV-B radiation of CYR31 urediospores is more than that of CYR32 and CYR33, indicating that UV-B radiation has different biological effects on different *Pst* physiological races, and different *Pst* physiological races have different reaction mechanisms for UV-B radiation. The functions of DEP were classified into "information storage and processing", "cellular processes and signaling", "metabolism" and "poorly characterized" in this study. All poorly characterized proteins sub-divided into "general function prediction only" or "function unknown",

Table 2: Down-regulated differentially expressed proteins in the urediospores of the three *Pst* physiological races including CYR31, CYR32 and CYR33 after UV-B radiation

COG functional classification	Accession	Description	Treatment combination	Fold change
Information storage and processing				
[A]RNA processing and modification	E3JZI5	Putative uncharacterized protein	CYR33LD$_{90}$ VS CYR33CK	0.58
	J3Q5E8	Uncharacterized protein	CYR32LD$_{90}$ VS CYR32CK	0.53
	W4KPP8	Uncharacterized protein	CYR33LD$_{90}$ VS CYR33CK	0.53
[B]Chromatin structure and dynamics	E3KBG2	Putative uncharacterized protein	CYR32LD$_{90}$ VS CYR32CK	0.49
	E6R1E4	Histone H2A	CYR33LD$_{90}$ VS CYR33CK	0.40
	M5FWC9	Histone H2A	CYR33LD$_{90}$ VS CYR33CK	0.47
[J]Translation, ribosomal structure and biogenesis	A8PX11	Putative uncharacterized protein	CYR31LD$_{90}$ VS CYR31CK	0.51
			CYR33LD$_{90}$ VS CYR33CK	0.57
	C0K1C3	Transcription elongation factor 1-alpha (Fragment)	CYR33LD$_{90}$ VS CYR33CK	0.56
	D1MWJ6	Translation elongation factor 1-alpha (Fragment)	CYR31LD$_{90}$ VS CYR31CK	0.52
	E6RA36	60S acidic ribosomal protein, putative	CYR33LD$_{90}$ VS CYR33CK	0.65
	E7A0U5	Probable ribosomal protein S4.e, cytosolic	CYR32LD$_{90}$ VS CYR32CK	0.57
	F1B370	Translation elongation factor 1-alpha (Fragment)	CYR33LD$_{90}$ VS CYR33CK	0.50
	G2ZGA9	Elongation factor 1 (Fragment)	CYR32LD$_{90}$ VS CYR32CK	0.64
	I4YGJ3	Ribosomal protein L15	CYR31LD$_{90}$ VS CYR31CK	0.55
			CYR33LD$_{90}$ VS CYR33CK	0.42
	I4Y6G4	Elongation factor 1-alpha	CYR33LD$_{90}$ VS CYR33CK	0.55
	P51997	60S ribosomal protein L25	CYR33LD$_{90}$ VS CYR33CK	0.50
	U3L266	Elongation factor 1-alpha (Fragment)	CYR33LD$_{90}$ VS CYR33CK	0.58
[L]Replication, recombination and repair	E3KKF8	Putative uncharacterized protein	CYR32LD$_{90}$ VS CYR32CK	0.34
	E3KQ21	Peptidyl-prolyl cis-trans isomerase	CYR32LD$_{90}$ VS CYR32CK	0.48
	J3Q7H7	Uncharacterized protein	CYR31LD$_{90}$ VS CYR31CK	0.47
	J3QBG8	Uncharacterized protein	CYR32LD$_{90}$ VS CYR32CK	0.66
	J3Q9A2	Uncharacterized protein	CYR33LD$_{90}$ VS CYR33CK	0.37
	P87036	Heat shock protein 70	CYR31LD$_{90}$ VS CYR31CK	0.11
Cellular processing and signaling				
[U]Intracellular trafficking, secretion, and vesicular transport	E3JT80	Putative uncharacterized protein	CYR32LD$_{90}$ VS CYR32CK	0.62
	E3L2E7	Putative uncharacterized protein	CYR33LD$_{90}$ VS CYR33CK	0.38
	E3KTV7	Putative uncharacterized protein	CYR33LD$_{90}$ VS CYR33CK	0.65
[Z]Cytoskeleton	B0LC31	Beta-tubulin 1 (Fragment)	CYR31LD$_{90}$ VS CYR31CK	0.61
	F4RAK2	Putative uncharacterized protein	CYR31LD$_{90}$ VS CYR31CK	0.60
			CYR33LD$_{90}$ VS CYR33CK	0.40
	F4S614	Putative uncharacterized protein	CYR33LD$_{90}$ VS CYR33CK	0.63
	G7DSE9	Uncharacterized protein	CYR31LD$_{90}$ VS CYR31CK	0.36
	Q2IAP9	Beta-tubulin (Fragment)	CYR31LD$_{90}$ VS CYR31CK	0.49
			CYR33LD$_{90}$ VS CYR33CK	0.60
Metabolism				
[C]Energy production and conversion	D8V186	Cytochrome c oxidase subunit 2	CTR31LD$_{90}$ VS CYR31CK	0.49
	E3L4W6	Succinate-semialdehyde dehydrogenase (NADP$^+$)	CYR32LD$_{90}$ VS CYR32CK	0.33
	G7DS01	ATP synthase subunit alpha	CYR32LD$_{90}$ VS CYR32CK	0.63
	G7E585	Uncharacterized protein	CYR32LD$_{90}$ VS CYR32CK	0.65
	J3PS85	Uncharacterized protein	CYR32LD$_{90}$ VS CYR32CK	0.56
	W4K8P5	NADH:ubiquinone oxidoreductase	CYR32LD$_{90}$ VS CYR32CK	0.42
[E]Amino acid transport and metabolism	M7WMS7	5-oxoprolinase	CYR32LD$_{90}$ VS CYR32CK	0.28
[F]Nucleotide transport and metabolism	E3K2B0	Thymidylate kinase	CYR31LD$_{90}$ VS CYR31CK	0.60
			CYR32LD$_{90}$ VS CYR32CK	0.33
[G]Carbohydrate transport and metabolism	A8NNV3	Transaldolase	CYR32LD$_{90}$ VS CYR32CK	0.64
	L8X8P7	PfkB domain-containing protein	CYR31LD$_{90}$ VS CYR31CK	0.45
			CYR32LD$_{90}$ VS CYR32CK	0.47
	Q5I5F8	Glyceraldehyde 3-phosphate dehydrogenase (Fragment)	CYR32LD$_{90}$ VS CYR32CK	0.61
	S7PV39	Transaldolase	CYR32LD$_{90}$ VS CYR32CK	0.61
[H]Coenzyme transport and metabolism	F4RPZ7	Putative uncharacterized protein	CYR31LD$_{90}$ VS CYR31CK	0.13
			CYR33LD$_{90}$ VS CYR33CK	0.57
Poorly characterized				
[R]General function prediction only	E6ZLC3	G-protein beta subunit Bpp1	CYR31LD$_{90}$ VS CYR31CK	0.64
	J3QFK7	Uncharacterized protein (Fragment)	CYR32LD$_{90}$ VS CYR32CK	0.58
[S]Function unknown	H6QUA0	Putative uncharacterized protein	CYR33LD$_{90}$ VS CYR33CK	0.65
No annotation	E3L419	Putative uncharacterized protein	CYR32LD$_{90}$ VS CYR32CK	0.64
	E3KKW7	Putative uncharacterized protein	CYR33LD$_{90}$ VS CYR33CK	0.66
	F4RAN1	Putative uncharacterized protein	CYR32LD$_{90}$ VS CYR32CK	0.50
	J3PZX9	Uncharacterized protein	CYR31LD$_{90}$ VS CYR31CK	0.42
	J3PRM2	Uncharacterized protein	CYR32LD$_{90}$ VS CYR32CK	0.66
	J3QJI5	Uncharacterized protein	CYR31LD$_{90}$ VS CYR31CK	0.50
	J3Q2H1	Uncharacterized protein	CYR32LD$_{90}$ VS CYR32CK	0.53
	J3QGG1	Uncharacterized protein	CYR31LD$_{90}$ VS CYR31CK	0.44
	V2YR52	Uncharacterized protein	CYR32LD$_{90}$ VS CYR32CK	0.34

were regarded as predicted or unknown proteins. Therefore, to better explain the differentially expressed proteins from the three physiological races of *Pst*, only DEP involved in the first three categories were discussed as follows.

In the UV-B irradiated urediospores of CYR31, the up-regulated translation elongation factor 1 alpha (A4KBU8), transcription elongation factor 1-alpha (C0K1C3), translation initiation factor eIF-4A (M7WTM4),

Table 3: KEGG pathway enrichment of differentially expressed proteins in the urediospores of the three *Pst* physiological races including CYR31, CYR32 and CYR33 after UV-B radiation

Pathway	Pathway ID	*P* value		
		CYR31LD$_{90}$ VS CYR31CK	CYR32LD$_{90}$ VS CYR32CK	CYR33LD$_{90}$ VS CYR33CK
Gap junction	ko04540	0.00242		
RNA transport	ko03013	0.01200		0.00055
Pathogenic Escherichia coli infection	ko05130	0.00344		0.00454
Ribosome	ko03010		0.01770	
Antigen processing and presentation	ko04612		0.02220	
Spliceosome	ko03040			0.00652
Systemic lupuserythematosus	ko05322			0.00296
Arrhythmogenic right ventricular cardiomyopathy (ARVC)	ko05412			0.03100
Hypertrophic cardiomyopathy (HCM)	ko05410			0.03100
Viral myocarditis	ko05416			0.03410
Dilated cardiomyopathy	ko05414			0.04330

translation elongation factor EF1-alpha (Q5EG81) and elongation factor 1-alpha (U3L266) were found to be involved in protein biogenesis. In the UV-B irradiated urediospores of CYR32, the up-regulated 60S ribosomal protein L36 (E3JQ18), ribosomal protein L15 (I4YGJ3) and 60S ribosomal protein l34-b (V2XVD8) are the components of the 60S subunit of the eukaryotic ribosome, which can play an important role in the initiation of complex assembly during the synthesis of peptide chains. The results indicated that ribosomal proteins may affect protein synthesis and assembly after UV-B radiation. In a study conducted by Zhao *et al*. (2016), the 60S ribosomal protein L22 (striiformis_Gene24126), 60S ribosomal protein L23 (striiformis_Gene15022) and 60S ribosomal protein L32 (striiformis_Gene20458) were down-regulated, which suggested that ribosomal proteins were mainly associated with the synthesis of proteins under normal physiological conditions. However, the up-regulated expression of ribosomal proteins after UV-B radiation of the *Pst* urediospores could result in the disordering of physiological processes. In the UV-B irradiated urediospores of CYR33, C0K1C3, translation elongation factor 1-alpha (F1B370), U3L266 and 60S ribosomal protein L25 (P51997) were down-regulated. The results described above indicated that UV-B radiation had some effects on the protein biosynthesis of *Pst* urediospores, but the effects had race-dependent differences.

DEP whose functions were classified into cellular processes and signaling were mainly involved in "cell wall/membrane/envelope biogenesis", "posttranslational modification, protein turnover, chaperones", "intracellular trafficking, secretion and vesicular transport", "cell cycle control, cell division, chromosome partitioning", and "cytoskeleton".

SCF ubiquitin ligase (A8NE72) is a component of the ubiquitin-proteasome system (UPS). It specifically recognizes the target protein; ubiquitin is attached to the target protein specific site and is finally degraded by the 26S proteasome (Ciechanover *et al*., 1984). In this study, the up-regulated expression of A8NE72 in the urediospores of CYR31 was induced by UV-B radiation, which may promote the degradation of proteins of the urediospores, resulting in cell death. An uncharacterized protein (K5WSF5) with catalytic activity for ubiquitin-like proteins was also up-regulated in the UV-B irradiated urediospores of CYR31 in this study. This further proved that the UV-B radiation promoted the UPS reaction which resulted in the death of the *Pst* urediospores.

In eukaryotes, the 14-3-3 protein (A7KJS2) is capable of binding to many target proteins associated with biological processes. Studies have shown that biotic and abiotic stresses can induce the expression of the 14-3-3 gene (Roberts *et al*., 2002; Li *et al*., 2015). In this study, the expression of A7KJS2 was increased in the UV-B irradiated urediospores of CYR31, indicating that UV-B radiation can induce the expression of the protein. However, the specific mechanism requires further study.

The main metabolic pathways in which the acquired DEP were involved were "energy production and conversion", "nucleotide transport and metabolism", and "carbohydrate transport and metabolism". Eighteen DEP were involved in the three metabolic pathways, of which seven proteins were up-regulated and 11 proteins were down-regulated. DEP were involved in the glycolysis/gluconeogenesis pathway, the pentose phosphate pathway (PPP) and the tricarboxylic acid (TCA) cycle. Phosphoglycerate kinase (PGK) (M7X689) and glyceraldehyde 3-phosphate dehydrogenase (GAPDH) (Q5I5F8) were associated with the glycolysis/gluconeogenesis pathway. PfkB domain-containing protein (L8X8P7) and transaldolase (A8NNV3) were associated with PPP. Since PGK is a pivotal enzyme in the glycolytic pathway, function reduction or loss of PGK resulting from PGK gene mutations can have a great impact on the survival of a living organism. Joshi *et al*. (2016) reported that the expression of four PGK genes (OsPgks) encoding phosphoglycerate kinase in rice was induced under salt stress, which could enhance the resistance of rice to salt stress. UV-B radiation is a type of abiotic stress as well as salt stress. In the UV-B irradiated urediospores of CYR33, the expression of M7X689 was up-regulated, suggesting that this may be a defense response of *Pst*

urediospores to adapt to stress. A study conducted by Ferreira *et al*. (2015) showed that GAPDH could interact with uracil-DNA glycosylase and was involved in the repair of cytotoxic DNA lesions in *Escherichia coli*, indicating that GAPDH could play roles in the repair of DNA bases. In this study, the expression of Q5I5F8 was down-regulated in the UV-B irradiated urediospores of CYR32. This may be caused by damages to urediospore DNA, such as DNA mismatch induced by UV-B radiation that blocks the DNA repair mechanism in which GAPDH is involved.

In the UV-B irradiated urediospores of CYR31, the expression of isocitrate dehydrogenase (IDH) (E3K6X4), an important enzyme in the TCA cycle, was up-regulated. Up-regulated expression of IDH can promote the production of NADH and ATP. NADH produces electrons that are then transported to O_2, which is accompanied by the generation of large amounts of energy, and the proton gradient that is simultaneously formed can drive the synthesis of ATP (Lin *et al*., 2001). In addition, the up-regulated expression of NADH:ubiquinone oxidoreductase (complex I) (W4K8P5) in the electron transport chain can increase the electron transfer. However, the expression of the cytochrome c oxidase subunit 2 (complex IV) (D8V186) was down-regulated in this study, indicating that the activity of cytochrome c oxidase in the electron transport chain was inhibited after UV-B radiation. Thus, electrons could not be transferred to O_2 and the synthesis of ATP was inhibited. The organic compounds could not be synthesized normally, resulting in the accelerated death of urediospores. In the UV-B irradiated urediospores of CYR32, the expression of E3K6X4 was up-regulated, indicating that the synthesis of ATP was also inhibited. In the study conducted by Zhao *et al*. (2016), the NADH-ubiquinone oxidoreductase subunit (striiformis_Gene10701), ATP synthase subunit beta (striiformis_Gene27232) and ATP synthase subunit gamma (striiformis_Gene21422) were up-regulated, indicating that ATP metabolism was promoted during the urediospore germination. However, the expression of ATP-related enzymes was down-regulated in the *Pst* urediospores after UV-B radiation in this study, indicating that the metabolic process of ATP was inhibited. In the UV-B irradiated urediospores of CYR33, there were no significant differences in the expression of these proteins, and UV-B radiation had more effects on the energy metabolism of urediospores of CYR31 and CYR32. It can be inferred that CYR33 may have more potential to survive in external environments to become a dominant physiological race, consistent with the monitoring results of *Pst* in recent years in China (Wan *et al*., 2003; Wang *et al*., 2007; Jia *et al*., 2011; Li *et al*., 2012).

Moreover, the expression of proteins in fungi may be affected by other abiotic stresses such as nutritional stress (Yang and Yin, 2016), water stress (Ghabooli *et al*., 2013), and drought stress (Kerner *et al*., 2012). Further studies into the proteomic changes of *Pst* urediospores caused by other abiotic stresses should be conducted to understand the virulence variation mechanisms of *Pst*.

Conclusion

A total of 2,136 proteins were identified from the *Pst* urediospores before and after UV-B radiation. Compared to the corresponding controls, 43, 45 and 35 proteins were differentially expressed in the UV-B irradiated urediospores of CYR31, CYR32 and CYR33, respectively. Among these DEP, 26, 20 and 14 proteins were up-regulated and 17, 25 and 21 proteins were down-regulated in the UV-B irradiated urediospores of CYR31, CYR32 and CYR33, respectively. DEP were mainly involved in energy metabolism, substance metabolism and DNA biosynthesis. This study can play a useful role in understanding the virulence variation mechanisms of *Pst* caused by UV-B radiation.

Acknowledgements

This study was supported by National Key Basic Research Program of China (Grant Number: 2013CB127700) and National Natural Science Foundation of China (Grant Number: 31101393).

References

Braga, G.U.L., D.E.N. Rangel, É.K.K. Fernandes, S.D. Flint and D.W. Roberts, 2015. Molecular and physiological effects of environmental UV radiation on fungal conidia. *Curr. Genet*., 61: 405–425

Briolant, S., L. Almeras, M. Belghazi, E. Boucomont-Chapeaublanc, N. Wurtz, A. Fontaine, S. Granjeaud, T. Fusaï, C. Rogier and B. Pradines, 2010. *Plasmodium falciparum* proteome changes in response to doxycycline treatment. *Malar. J*., 9: 141

Brosché, M. and Å. Strid, 2000. Ultraviolet-B radiation causes tendril coiling in *Pisum sativum*. *Plant Cell Physiol*., 41: 1077–1079

Chen, W.Q., C. Wellings, X.M. Chen, Z.S. Kang and T.G. Liu, 2014. Wheat stripe (yellow) rust caused by *Puccinia striiformis* f. sp. *tritici*. *Mol. Plant Pathol*., 15: 433–446

Cheng, P., Z.H. Ma, X.J. Wang, C.Q. Wang, Y. Li, S.H. Wang and H.G. Wang, 2014. Impact of UV-B radiation on aspects of germination and epidemiological components of three major physiological races of *Puccinia striiformis* f. sp. *tritici*. *Crop Prot*., 65: 6–14

Ciechanover, A., D. Finley and A. Varshavsky, 1984. The ubiquitin-mediated proteolytic pathway and mechanisms of energy-dependent intracellular protein degradation. *J. Cell. Biochem*., 24: 27–53

Conesa, A., S. Götz, J.M. García-Gómez, J. Terol, M. Talón and M. Robles, 2005. Blast2GO: a universal tool for annotation, visualization and analysis in functional genomics research. *Bioinformatics*, 21: 3674–3676

Cooper, B., A. Neelam, K.B. Campbell, J. Lee, G. Liu, W.M. Garrett, B. Scheffler and M.L. Tucker, 2007. Protein accumulation in the germinating *Uromyces appendiculatus* uredospore. *Mol. Plant Microb. Interact*., 20: 857–866

Costa, L.B., D.E.N. Rangel, M.A.B. Morandi and W. Bettiol, 2012. Impact of UV-B radiation on *Clonostachys rosea* germination and growth. *World J. Microb. Biotechnol*., 28: 2497–2504

Cuadra, P., D. Vargas, V. Fajardo and R. Herrera, 2010. Effects of UV-B radiation in morpho-genetic characters of *Gnaphalium luteo-album*. *J. Photochem. Photobiol. B*, 101: 70–75

Demirci, Y.E., C. Inan, A. Günel, D. Maytalman, Z. Mert, A.T. Baykal, S.V. Korkut, N. Arda and S. Hasancebi, 2016. Proteome profiling of the compatible interaction between wheat and stripe rust. *Eur. J. Plant Pathol*., 145: 941–962

Ferreira, E., R. Giménez, M.A. Cañas, L. Aguilera, J. Aguilar, J. Badia and L. Baldomà, 2015. Glyceraldehyde-3-phosphate dehydrogenase is required for efficient repair of cytotoxic DNA lesions in *Escherichia coli*. *Int. J. Biochem. Cell B.*, 60: 202–212

Fourtouni, A., Y. Manetas and C. Christias, 1998. Effects of UV-B radiation on growth, pigmentation, and spore production in the phytopathogenic fungus *Alternaria solani*. *Can. J. Bot.*, 76: 2093–2099

Fu, Y., H. Zhang, S.N. Mandal, C.Y. Wang, C.H. Chen and W.Q. Ji, 2016. Quantitative proteomics reveals the central changes of wheat in response to powdery mildew. *J. Proteom.*, 130: 108–119

Ghabooli, M., B. Khatabi, F.S. Ahmadi, M. Sepehri, M. Mirzaei, A. Amirkhani, J.V. Jorrín-Novo and G.H. Salekdeh, 2013. Proteomics study reveals the molecular mechanisms underlying water stress tolerance induced by *Piriformospora indica* in barley. *J. Proteom.*, 94: 289–301

Huang, L.L., X.L. Wang, Z.S. Kang and J. Zhao, 2005. Mutation of pathogenicity induced by ultraviolet radiation in *Puccinia striiformis* f. sp. *tritici* and RAPD analysis of mutants. *Mycosystema*, 24: 400–406

Inostroza-Blancheteau, C., M. Reyes-Díaz, A. Arellano, M. Latsague, P. Acevedo, R. Loyola, P. Arce-Johnson and M. Alberdi, 2014. Effects of UV-B radiation on anatomical characteristics, phenolic compounds and gene expression of the phenylpropanoid pathway in highbush blueberry leaves. *Plant Physiol. Biochem.*, 85: 85–95

Jia, Q.Z., S.L. Jin, S.Q. Cao, H.S. Lou, J. Huang, B. Zhang and M.A. Jin, 2011. Monitoring results of physiologic races of wheat stripe rust in Gansu Province during 2008-2009. *Plant Prot.*, 37: 130–133

Jing, J.X., H.S. Shang and Z.Q. Li, 1993. The biological effects of ultraviolet ray radiation on wheat stripe rust (*Puccinia striiformis* West.). *Acta Phytopathol. Sin.*, 23: 299–304

Joshi, R., R. Karan, S.L. Singla-Pareek and A. Pareek, 2016. Ectopic expression of Pokkali phosphoglycerate kinase-2 (OsPGK2-P) improves yield in tobacco plants under salinity stress. *Plant Cell Rep.*, 35: 27–41

Kang, Z.S., X.J. Wang, J. Zhao, C.L. Tang and L.L. Huang, 2015. Advances in research of pathogenicity and virulence variation of the wheat Stripe rust fungus *Puccinia striiformis* f. sp. *tritici*. *Sci. Agric. Sin.*, 48: 3439–3453

Kerner, R., E. Delgado-Eckert, E. Del Castillo, G. Müller-Starck, M. Peter, B. Kuster, E. Tisserant and K. Pritsch, 2012. Comprehensive proteome analysis in *Cenococcum geophilum* Fr. as a tool to discover drought-related proteins. *J. Proteom.*, 75: 3707–3719

Kramer, A., H.C. Beck, A. Kumar, L.P. Kristensen, J.F. Imhoff and A. Labes, 2015. Proteomic analysis of anti-cancerous scopularide production by a marine *Microascus brevicaulis* strain and its UV mutant. *PLoS One*, 10: e0140047

Li, Q., G.B. Li, B.T. Wang, F. Wang and Z.S. Kang, 2012. Pathogenic changes of the stripe rust fungus of wheat in Shaanxi Province during 2006–2010. *Plant Prot.*, 38: 133–136

Li, R.H., X.T. Jiang, D.H. Jin, S. Dhaubhadel, S.M. Bian and X.Y. Li, 2015. Identification of 14-3-3 family in common bean and their response to abiotic stress. *PLoS One*, 10: e0143280

Li, Z.Q. and S.M. Zeng, 2002. *Wheat Rusts Rusts in China*. China Agriculture Press, Beijing, China

Liang, G.Y., H.L. Ji, Z.Y. Zhang, H.T. Wei, Z.S. Kang, Y.L. Peng and Y.J. Li, 2007. Proteome analysis of slow-rusting variety Chuanmai 107 inoculated by wheat stripe rust (*Puccina striiformis*). *J. Trit. Crops*, 27: 335–340

Lin, A.P., M.T. McCammon and L. McAlister-Henn, 2001. Kinetic and physiological effects of alterations in homologous isocitrate-binding sites of yeast NAD^+-specific isocitrate dehydrogenase. *Biochemistry*, 40: 14291–14301

Line, R.F., 2002. Stripe rust of wheat and barley in North America: a retrospective historical review. *Annu. Rev. Phytopathol.*, 40: 75–118

Luster, D.G., M.B. McMahon, M.L. Carter, L.L. Fortis and A. Nunez, 2010. Proteomic analysis of germinating urediniospores of *Phakopsora pachyrhizi*, causal agent of Asian soybean rust. *Proteomics*, 10: 3549–3557

Ma, C., S.C. Xu, Q. Xu, Z.H. Zhang and Y.H. Pan, 2009. Proteomic analysis of stripe rust resistance wheat line Taichung29*6/*Yr5* inoculated with stripe rust race CY32. *Sci. Agric. Sin.*, 42: 1616–1623

Manning, W.J. and A. Tiedemann, 1995. Climate change: Potential effects of increased atmospheric carbon dioxide (CO_2), ozone (O_3) and ultraviolet-B (UV-B) radiation on plant diseases. *Environ. Pollut.*, 88: 219–245

Maytalman, D., Z. Mert, A.T. Baykal, C. Inan, A. Günel and S. Hasancebi, 2013. Proteomic analysis of early responsive resistance proteins of wheat (*Triticum aestivum)* to yellow rust (*Puccinia striiformis* f. sp. *tritici*) using ProteomeLab PF2D. *Plant Omics J.*, 6: 24–35

Pandey, A. and M. Mann, 2000. Proteomics to study genes and genomes. *Nature*, 405: 837–846

Redding, A.M., A. Mukhopadhyay, D.C. Joyner, T.C. Hazen and J.D. Keasling, 2006. Study of nitrate stress in Desulfovibrio vulgaris Hildenborough using iTRAQ proteomics. *Brief. Funct. Genom. Proteom.*, 5: 133–143

Roberts, M.R., J. Salinas and D.B. Collinge, 2002. 14-3-3 proteins and the response to abiotic and biotic stress. *Plant Mol. Biol.*, 50: 1031–1039

Rosen, R., A.G. Matthysse, D. Becher, D. Biran, T. Yura, M. Hecker and E.Z. Ron, 2003. Proteome analysis of plant-induced proteins of *Agrobacterium tumefaciens*. *FEMS Microbiol. Ecol.*, 44: 355–360

Shang, H.S., J.X. Jing and Z.Q. Li, 1994. Mutations induced by ultraviolet radiation affecting virulence in *Puccinia striiformis*. *Acta Phytopathol. Sin.*, 24: 347–351

Teramura, A.H. and J.H. Sullivan, 1994. Effects of UV-B radiation on photosynthesis and growth of terrestrial plants. *Photosynth. Res.*, 39: 463–473

Trentin, A.R., M. Pivato, S.M.M. Mehdi, L.E. Barnabas, S. Giaretta, M. Fabrega-Prats, D. Prasad, G. Arrigoni and A. Masi, 2015. Proteome readjustments in the apoplastic space of *Arabidopsis thaliana ggt1* mutant leaves exposed to UV-B radiation. *Front. Plant Sci.*, 6: 128

Wan, A.M., L.R. Wu, Q.Z. Jia, S.L. Jin, G.B. Li, B.T. Wang, G. Yao, J.X. Yang, Z.Y. Yuan and Y.Q. Bi, 2003. Pathogenic changes of stripe rust fungus of wheat in China during 1997–2001. *Acta Phytopathol. Sin.*, 33: 261–266

Wang, B.T., G.B. Li, Q. Li, F. Wang and Z.S. Kang, 2007. Population changes of stripe rust fungus of wheat in Shaanxi province during 2001-2005. *J. Northwest A. F. Univ.* (*Nat. Sci. ed.*), 35: 209–216

Wang, X.J., Z.H. Ma, Y.Y. Jiang, S.D. Shi, W.C. Liu, J. Zeng, Z.W. Zhao and H.G. Wang, 2014. Modeling of the overwintering distribution of *Puccinia striiformis* f. sp. *tritici* based on meteorological data from 2001 to 2012 in China. *Front. Agric. Sci. Eng.*, 1: 223–235

Wang, X.L., F. Zhu, L.L. Huang, G.R. Wei and Z.S. Kang, 2009. Effects of ultraviolet radiation on pathogenicity mutation of *Puccinia striiformis* f. sp. *tritici*. *J. Nucl. Agric. Sci.*, 23: 375–379

Willocquet, L., D. Colombet, M. Rougier, J. Fargues and M. Clerjeau, 1996. Effects of radiation, especially ultraviolet B, on conidial germination and mycelial growth of grape powdery mildew. *Eur. J. Plant Pathol.*, 102: 441–449

Wu, S.T., Z.W. Zhu, L.M. Fu, B.F. Niu and W.Z. Li, 2011. WebMGA: a customizable web server for fast metagenomic sequence analysis. *BMC Genom.*, 12: 444

Yang, F. and Q. Yin, 2016. Comprehensive proteomic analysis of the wheat pathogenic fungus *Zymoseptoria tritici*. *Proteomics*, 16: 98–101

Yang, Y.H., Y. Yu, C.W. Bi and Z.S. Kang, 2016. Quantitative proteomics reveals the defense response of wheat against *Puccinia striiformis* f. sp. *tritici*. *Sci. Rep.*, 6: 34261

Zhao, J., H. Zhuang, G.M. Zhan, L.L. Huang and Z.S. Kang, 2016. Proteomic analysis of *Puccina striiformis* f. sp. *tritici* (*Pst*) during uredospore germination. *Eur. J. Plant Pathol.*, 144: 121–132

Zhu, M.M., B. Simons, N. Zhu, D.G. Oppenheimer and S.X. Chen, 2010. Analysis of abscisic acid responsive proteins in *Brassica napus* guard cells by multiplexed isobaric tagging. *J. Proteom.*, 73: 790–805

(Received 09 January 2018; Accepted 13 April 2018)